BIOCHEMISTRY
including biophysical chemistry & molecular biology

Article

pubs.acs.org/biochemistry

A Kinetic Analysis of the Folding and Unfolding of OmpA in Urea and Guanidinium Chloride: Single and Parallel Pathways

Kell K. Andersen, Huabing Wang, and Daniel E. Otzen*

Interdisciplinary Nanoscience Centre (iNANO), Centre for Insoluble Protein Structures (inSPIN), Department of Molecular Biology and Genetics, University of Aarhus, Gustav Wieds Vej 14, DK-8000 Aarhus C, Denmark

Supporting Information

ABSTRACT: The outer membrane protein OmpA from *Escherichia coli* can fold into lipid vesicles and surfactant micelles from the urea-denatured state. However, a complete kinetic description of the folding and unfolding of OmpA, which can provide the basis for subsequent protein engineering studies of the protein's folding pathway, is lacking. Here we use two different denaturants to probe the unfolding mechanism of OmpA in the presence of the surfactant octyl maltoside (OM). Unfolding of OmpA in the presence of micelles, achieved with the potent denaturant guanidinium chloride (GdmCl), leads to single-phase unfolding. In contrast, OmpA unfolds in urea only below OM's critical micelle concentration, and this occurs in different phases, which we attribute to the existence of states that have bound different amounts of surfactant, from completely "naked" to partly covered by surfactant. Multiple parallel refolding phases are attributed to different levels of collapse prior to folding. Kinetic results used to derive the stability of OmpA in surfactant, using either urea or GdmCl as the denaturing agent, give comparable results and indicate a minimalist three-state folding scheme involving denatured state D, folding intermediate I, and native state N. N and I are stabilized by 15.6 and 2.6 kcal/mol, respectively, relative to D. The periplasmic domain of OmpA does not contribute to stability in surfactant micelles. However, BBP, a minimalist transmembrane β-barrel version of OmpA with shortened loops, is destabilized by ~10 kcal/mol compared to OmpA, highlighting loop contributions to OmpA stability.

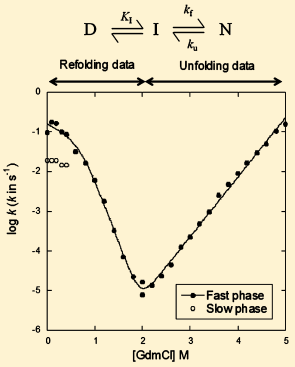

Bacterial outer membrane proteins (OMPs) make up a diverse group of β-barrel proteins, including adhesins, architectural proteins, passive diffusion pores, siderophore receptors, efflux channels, protein translocation pores, and enzymes, e.g., lipases, proteases, and palmitoyl transferases.[1] Their many functions are conducted with a very simple structural framework consisting of typically 8−16 β-strands. Whereas α-helical membrane proteins often have long unbroken sequences of highly hydrophobic residues in their helical transmembrane segments, OMP transmembrane β-strands typically consist of alternating hydrophilic and hydrophobic residues. This reduces their overall hydrophobicity and in practice makes it possible to refold many of them from the urea-denatured state by dilution in the presence of phospholipid vesicles or surfactant micelles.[2] The outer bacterial membrane is an asymmetric bilayer in which the outer and inner leaflets vary considerably in composition. The inner leaflet contains a large proportion of phospholipids, whereas the outer leaflet is dominated by lipopolysaccharide (LPS). Manufacturing vesicles with such an asymmetric distribution of phospholipids and LPS is not simple, and hence, vesicles composed entirely of phospholipids are usually used as model systems in folding studies of membrane proteins.

The most detailed OMP folding studies have been performed on the highly abundant OmpA from *Escherichia coli*, a two-domain OMP whose 171-residue N-terminal domain forms an eight-stranded β-barrel embedded in the outer membrane. Although the structure of the 154-residue C-terminal domain has not yet been determined despite ongoing efforts,[3] a homologous domain from protein RmpM from *Neisseria meningitidis* with a 35% identical sequence shows mixed α- and β-structures.[4] With the pioneering studies of Surrey and Jähnig[5,6] and the elegant kinetic analyses by Kleinschmidt, Tamm, and co-workers[7−11] as a starting point, it has been shown that the N-terminal domain of OmpA inserts from the urea-unfolded state into small unilamellar vesicles in a series of steps. Hong and Tamm determined the free energy of unfolding ($\Delta G_{D\text{-}N}$) of OmpA at high pH and 37 °C in different phospholipid membranes to be 3−7 kcal/mol (depending on the lipid used), which lies at the low end of the range of 5−15 kcal/mol usually observed for water-soluble proteins.[12]

At present, kinetic studies of the folding and unfolding of OmpA in lipid vesicles have not proved to be tractable because of the extremely long time scales involved, and there are serious challenges with the reversible folding and unfolding of OmpA in vesicles (data not shown). Because OmpA is a flagship for the class of outer membrane proteins, it is of great interest to find appropriate conditions for reversible folding and unfolding on experimentally feasible time scales. One such option is provided by the replacement of lipids with surfactants.

Received: July 20, 2012
Revised: September 19, 2012
Published: September 19, 2012

Surfactants are amphiphilic surface active compounds that at concentrations above the critical micelle concentration (cmc) aggregate into supramolecular assemblies termed micelles. They are useful tools for studying membrane proteins because of their high solubility, ease of handling, and ability to form mixed micelles between nonionic and anionic surfactants with variable denaturing potency.[13,14] Surfactant micelles provide a hydrophobic environment that can facilitate folding of OMPs[15] and thus, in combination with chemical denaturants, provide a complete description of these proteins' mechanisms of folding and unfolding, using the approaches developed for water-soluble proteins such as analysis of chevron plots and protein engineering.[12] For such an approach to be successful, OMPs must fold and unfold reversibly over a wide range of denaturant concentrations. For many OMPs under a variety of conditions, N and D do not equilibrate in surfactants at the experimentally accessible time scale in the transition region where they are both significantly populated.[16] This leads to the phenomenon of hysteresis, where denaturation curves obtained using the denatured or native state as starting points do not overlap. A few exceptions have been reported. For example, the outer membrane lipase OmpLA undergoes completely reversible equilibrium unfolding in DLPC vesicles if the pH is kept below 4.0 and the protein is prevented from aggregation by low concentrations of the surfactant SB3-14 [3-(*N*,*N*-dimethylmyristylammonio)propanesulfonate].[17] Another example is provided by the folding of the OMP PagP into lipid vesicles, where an equilibrium between N and D could be established at very high urea concentrations, allowing two-state folding−unfolding kinetics to be observed within a relatively narrow urea concentration range (~7−10 M). This provided the basis for an elegant protein engineering analysis of the transition state of folding.[18] However, folding was more complicated at lower urea concentrations, involving several phases, and no comprehensive kinetic analysis of OMP folding and unfolding over the entire accessible urea concentration range has been reported to the best of our knowledge.

OmpA does not equilibrate completely between D and N on a time scale of days to weeks when unfolding the protein in urea. Here we show that the complete folding reversibility of OmpA may be achieved in the presence of the more potent denaturant guanidinium chloride (GdmCl), and that folding and unfolding occur sufficiently rapidly in this denaturant to allow us to collect kinetic data over the entire GdmCl concentration range spanning folding and unfolding. This allows us to construct a minimalist folding scheme for OmpA involving a single folding intermediate. Armed with this information, we have investigated the behavior of OmpA in urea. Unfolding and refolding rates for OmpA can be measured between 0 and 9 M urea, except for the range of 3.5−5.5 M urea, where kinetics were too slow to be measured on the experimentally accessible time scale. However, extrapolation of kinetic data to this region led to stability values comparable to those from GdmCl and furthermore revealed parallel folding−unfolding pathways, which are more pronounced in urea than in GdmCl. We conclude that OmpA can fold and unfold in parallel pathways starting from states collapsed to various extents, but "fast track" refolding and unfolding (which dominates in GdmCl) involve only D, an intermediate, and N. The periplasmic domain does not interfere with the folding of the transmembrane domain, while shortening of the extracellular loops to generate a minimal β-barrel structure strongly destabilizes the protein but does not alter the fundamental features of this folding pathway. This work provides the basis for subsequent protein engineering analysis of the folding−unfolding pathway of OmpA.

MATERIALS AND METHODS

Cloning of FL-OmpA. Full-length OmpA (termed FL-OmpA and encompassing residues 46−370 of the full sequence and excluding the first 45 residues that constitute the signal peptide) was expressed in cytoplasmic inclusion bodies in *E. coli* BL21(DE3) cells. To express OmpA, the gene was amplified via polymerase chain reaction from *E. coli* K12 genomic DNA. The two primers, 5′-gggaattc**catatg**gctccgaaagataacacacctg-3′ and 5′-ggccc**aagctt***tta*ttaagcctgcctgcggctgagttac-3′, were designed to amplify the sequence omitting the signal peptide and to introduce the gene between the NdeI and HindIII sites in the pET-3a vector (Stratagene). In the modified vector now designated pOmpAA, expression of the gene is under control of the T7 promoter. Transmembrane OmpA (termed TM-OmpA) and β-barrel platform (BBP) were expressed and purified in 8 M urea from inclusion bodies as described previously.[19,20] The vector for BBP was kindly provided by K. Pervushin.

Expression and Purification of FL-OmpA. pOmpAA was transformed into *E. coli* BL21(DE3) cells by heat shock treatment. Expression of OmpA was induced at an OD_{600} of 0.5 via the addition of 0.5 mM isopropyl β-D-thiogalactopyranoside, after which the culture was grown for 4 h and the cell pellet was harvested by centrifugation. Cells were resuspended in PBS buffer (20 mL/L of medium), and inclusion bodies were released from cells by ultrasound treatment with a Labsonic L Sonicator (Satorius BBI Systems). Sonication was performed with a 30 s on−off cycle 30 times in an ice-cold water bath. Inclusion bodies were collected by centrifugation and washed overnight in TEN buffer [50 mM Tris (pH 8), 1 mM EDTA, and 100 mM NaCl] containing 2% Triton X-100 (8 mL/L of culture). The next day inclusion bodies were collected by centrifugation and washed in TEN buffer without Triton X-100 for 2 h. Inclusion bodies were collected by centrifugation and dissolved in TN buffer containing 8 M urea. Insoluble impurities were removed by ultracentrifugation (45000*g* for 30 min). Urea-dissolved OmpA was prepared for anion exchange chromatography by dialysis against 50 volumes of 20 mM Tris (pH 9) and 8 M urea. Purification was conducted as described by Surrey et al.[21] with minor modifications using a 17 mL Source 15Q (GE Healthcare) column equilibrated with 20 mM Tris (pH 9.0) and 8 M urea. Fractions containing OmpA in 8 M urea were pooled, concentrated with Centricon Centrifugal Filter Units (Millipore, Billerica, MA), and stored at −80 °C. Sodium dodecyl sulfate−polyacrylamide gel electrophoresis (SDS−PAGE) analysis showed >95% purity, and the final concentration was 160 μM as determined by absorbance at 280 using a molar extinction coefficient of 50330 M^{-1} cm^{-1}.

Equilibrium Folding of OmpA in OM with Urea and GdmCl. For unfolding experiments in urea, OmpA was initially folded by dilution of 160 μM OmpA in 8 M urea 12.8-fold into 0.625 M urea, 55 mM octyl maltoside (OM), and glycine buffer [10 mM glycine (pH 10) and 2 mM EDTA] and incubation for 2 days at 37 °C. Appropriate amounts of glycine buffer and 55 mM OM with and without 10 M urea were mixed and diluted 4:1 with folded OmpA (final protein concentration of 2.5 μM). Solutions were incubated at 25 °C over several days, and samples were analyzed by SDS−PAGE without being boiled. The fraction of folded OmpA was evaluated by densitometry

dx.doi.org/10.1021/bi300974y | *Biochemistry* 2012, 51, 8371−8383

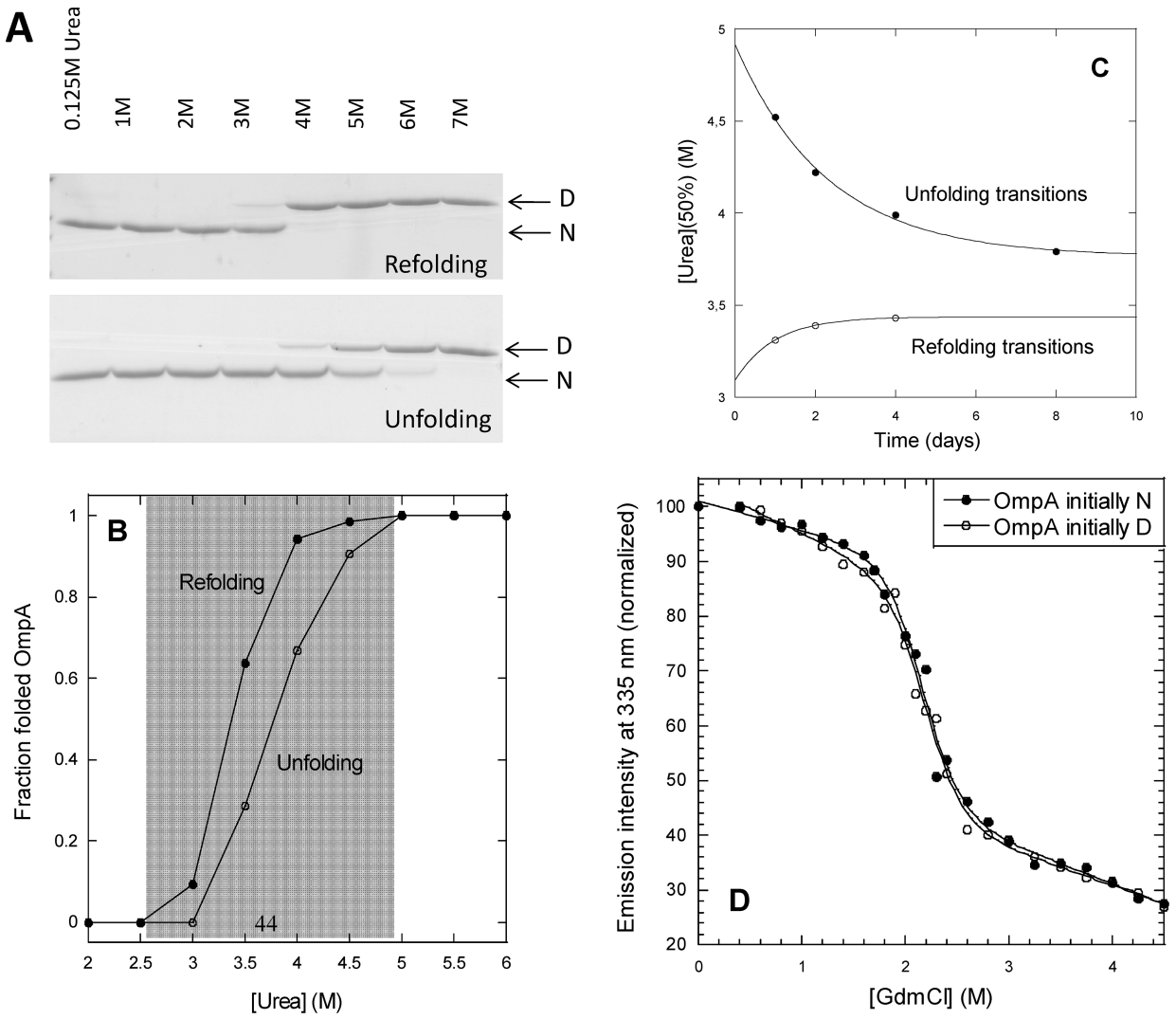

Figure 1. (A) Degrees of refolding and unfolding of OmpA in 55 mM OM at different concentrations of urea after incubation for 8 days. The reaction was followed by SDS–PAGE. OmpA was refolded from 8 M urea by dilution to different urea concentrations. OmpA was unfolded by first being refolded to 0.625 M urea and then transferred to higher urea concentrations. (B) Relative band intensities in panel A plotted vs urea concentration. The gray zone indicates the region of hysteresis between refolding and unfolding. (C) Midpoints of refolding and unfolding of OmpA change over time. Refolding is not completely reversible in urea. The midpoint, defined as the concentration at which 50% of OmpA is folded, is obtained by interpolation of data in panel B. (D) Denaturation of OmpA in GdmCl starting from the refolded and unfolded states. The data are fit to a two-state unfolding process with midpoints of 2.16 ± 0.04 and 2.20 ± 0.04 M GdmCl starting from the N state and the D state, respectively; the corresponding values of $m_{D\text{-}N}$ (which describe the linear dependence of the equilibrium constant of unfolding log $K_{D\text{-}N}$ on GdmCl concentration) are 3.40 ± 0.53 and 3.73 ± 0.47 M^{-1}, respectively.

using ImageJ.[22] For refolding experiments, 160 μM unfolded OmpA in 8 M urea was mixed with glycine buffer, surfactant, and urea to final concentrations of 2.5 μM OmpA and 55 mM OM. The final concentrations of surfactant and OmpA were the same as for equilibrium unfolding experiments. Experiments in GdmCl were performed essentially the same way, except that they were conducted in 250 mM OM to ensure that we were above the cmc at all GdmCl concentrations. In addition, for refolding experiments, OmpA was first diluted 12.8-fold into 0.625 M urea and 2 M GdmCl, after which it was diluted an additional 5-fold to final concentrations of 2.5 μM OmpA, 250 mM OM, and 0.4–4.5 M GdmCl.

Folding Kinetics in OM. OmpA or TM-OmpA was folded in OM for 2 days as described for equilibrium folding experiments. Measurements were taken on a Cary-Varian Eclipse fluorimeter in a 10 mm quartz cuvette with magnet stirring. Excitation and emission wavelengths were 295 and 335 nm, respectively, and slit widths were 10 nm (an excitation wavelength of 295 nm removes essentially all contributions from the 12 Tyr residues also present in the periplasmic domain and detects fluorescence from only the five Trp residues in the transmembrane domain). In a typical unfolding experiment, 0.8 mL of surfactant in glycine buffer with an appropriate amount of urea was equilibrated at 25 °C using the instrument thermostat; 0.2 mL of folded OmpA was then quickly added, and unfolding of the protein was followed by fluorescence. Refolding experiments were conducted by equilibrating glycine buffer with 55 mM OM and an appropriate amount of urea in a cuvette. Concentrated and unfolded OmpA was then added, and refolding was followed by fluorescence. Similar FL-OmpA folding and unfolding experiments were also conducted in 250 mM OM and different concentrations of GdmCl. Kinetic signals were always

dx.doi.org/10.1021/bi300974y | *Biochemistry* 2012, 51, 8371–8383

monitored for time periods corresponding to at least four half-lives of the slowest phase.

RESULTS

OmpA Does Not Undergo Completely Reversible Unfolding in Urea in Surfactants. To identify conditions that would allow us to determine the stability of OmpA in surfactants, we initially incubated OmpA in 55 mM OM and different concentrations of the chemical denaturant urea at 25 °C. Urea has been the traditional denaturant used to maintain OmpA in the unfolded state prior to refolding into vesicles and surfactants[7,10] and to conduct denaturation in the presence of vesicles.[23] The degree of folding was ascertained by SDS–PAGE, because the unfolded state of OmpA migrates more slowly than N because of its greater hydrodynamic radius (Figure 1A). The high kinetic barrier between D and N means that native OmpA, once formed, does not unfold in SDS at room temperature.[24] The reversibility of unfolding was probed by starting from both N and D (Figure 1B). However, it is clear that even after 8 days, the two transitions in urea have not merged (Figure 1C), and there is distinct hysteresis in the whole unfolding region (2.5–5.0 M urea). Similar results were obtained when the process was followed by a change in OmpA's tryptophan fluorescence (data not shown). This indicated that the unfolding of OmpA has not reached equilibrium within the region where N and D are both populated to significant extents. An even greater extent of hysteresis was also observed, because of a low degree of unfolding, when we attempted to fold and unfold OmpA in urea in the presence of decyl maltoside and dodecyl maltoside (data not shown). These surfactants have significantly lower critical micelle concentrations (cmc) than octyl maltoside, suggesting that micelles might stabilize OmpA against unfolding in urea. Given that micelles are stabilized by the hydrophobic effect, denaturants such as urea that solubilize hydrophobic moieties[25,26] will destabilize micelles by solubilizing monomeric surfactant molecules and thus increase the critical micelle concentration. OM has a cmc of 20 mM in water, but the cmc increases linearly with urea and reaches 55 mM around 3.2 M urea (Figure S1 of the Supporting Information). Thus, OM micelles will not be present to any significant extent above 3.2 M urea, and indeed, we observe unfolding only above this urea concentration (Figure 1B). If the OM concentration is increased sufficiently to form micelles at high urea concentrations, no OmpA unfolding is observed (data not shown). Thus, micelles have to be dissolved to allow OmpA unfolding in urea.

The lack of complete equilibration and the need for micelle dissolution complicate unfolding of OmpA in urea. We sought to remedy this using the denaturant GdmCl.

GdmCl Leads to Complete Folding Reversibility of OmpA at Micellar OM Concentrations. GdmCl is a significantly stronger denaturant than urea; the disadvantage is that it coprecipitates with SDS, preventing SDS–PAGE analysis of unfolding. However, the denaturation process may be followed by Trp fluorescence. Control experiments with urea show that SDS–PAGE and Trp fluorescence lead to the same unfolding–folding kinetics; differences between rate constants determined by the two methods are less than 10% (Figure S2 of the Supporting Information). The cmc of OM in 6 M GdmCl is 200 mM. Accordingly, we used 250 mM OM and denaturation in 0–4.5 M GdmCl to ensure that OM micelles were present at all concentrations and thus justify a unifying analysis of the folding–unfolding mechanism. Gratifyingly, when OmpA is incubated with increasing concentrations of GdmCl over a period of 4 days (starting from the N or D state), the two transitions essentially superimpose (Figure 1D). Fitting the data to a two-state unfolding transition provides a midpoint of denaturation of 2.17 ± 0.04 or 2.20 ± 0.04 M GdmCl depending on whether OmpA is initially folded or unfolded, respectively. Thus, unfolding in GdmCl leads to complete equilibration between N and D in the presence of OM micelles and provides a benchmark for comparison with potentially more complex unfolding and refolding in urea.

Folding and Unfolding of OmpA in GdmCl Reveal a Three-State Mechanism. A kinetic analysis of the unfolding and refolding of OmpA in GdmCl, monitored by the change in Trp fluorescence over time, provides a more complete picture of the denaturation process, allowing us to identify transient intermediates that are not populated under equilibrium conditions. Folding kinetics were fit to two-exponential decays up to 0.4 M GdmCl, while only a single-exponential decay was required between 0.4 and 2 M GdmCl (Figure 2, inset). All

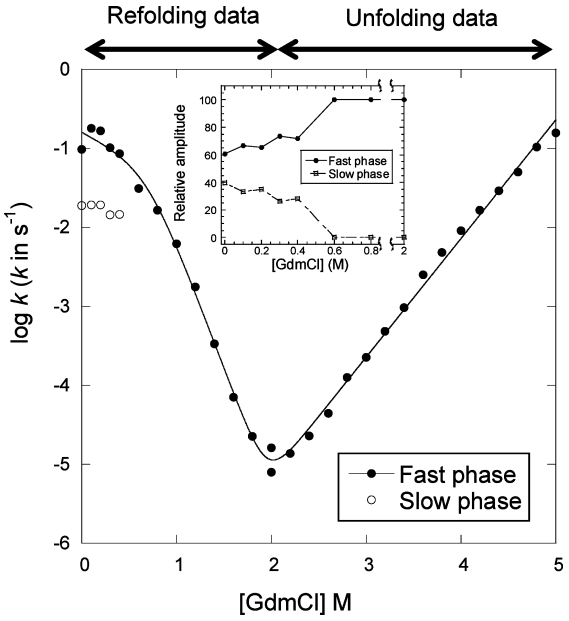

Figure 2. Folding and unfolding rate constants of FL-OmpA vs GdmCl concentration in 250 mM OM monitored by Trp fluorescence. Double phases are seen for folding at low GdmCl concentrations (up to 0.4 M). A single relaxation phase is seen for unfolding.

unfolding kinetics could be fit to a single-exponential decay over the entire unfolding range (2.0–5.0 M GdmCl). The unfolding and refolding rate constants obtained from these fits are plotted versus GdmCl concentration in Figure 2. The rate constants for the slow refolding phase are 1 order of magnitude lower than for the fast phase and are discussed below. The fast refolding rate constants in combination with the unfolding rate constants trace a V-shaped plot with a rollover at low GdmCl concentrations. Equilibration is extremely slow in the transition region, with half-lives of ~10^5 s to ~1 day (which means that several days are required to reach an equilibrium). Nevertheless, the refolding and unfolding rate constants overlap in the transition region (1.8–2.4 M GdmCl) and assume the same value around 2–2.1 M GdmCl, reasonably consistent with the midpoint of denaturation of ~2.2 M GdmCl from equilibrium

dx.doi.org/10.1021/bi300974y | Biochemistry 2012, 51, 8371–8383

Table 1. Summary of Kinetic Parameters Describing Folding and Unfolding of OmpA in Urea[a]

parameter[b]	FL-OmpA	TM-OmpA	BBP	FL-OmpA in GdmCl
$\log k_f^{water}$ (k in s^{-1})	−1.01 ± 0.04	−1.03 ± 0.18	−3.15 ± 0.09	−0.79 ± 0.08
m_f (M^{-1})	−0.38 ± 0.07	−0.31 ± 0.52	−0.19 ± 0.51	−0.61 ± 0.34
$\log K_I^{water}$	1.90 ± 0.12	1.42 ± 0.94	1.14 ± 0.52	1.78 ± 0.27
m_I (M^{-1})	−1.36 ± 0.06	−1.19 ± 0.33	−1.43 ± 0.32	−2.57 ± 0.27
$\log k_u^{water}$ (k in s^{-1})	−10.56 ± 0.31	−11.57 ± 0.89	−7.07 ± 0.17	−8.15 ± 0.12
m_u (M^{-1})	1.25 ± 0.04	1.41 ± 0.12	0.90 ± 0.03	1.50 ± 0.03
$\log K_{D\text{-}N}^{water}$[c]	11.46 ± 0.34	11.96 ± 1.31	5.06 ± 0.56	9.14 ± 0.31
$\Delta G_{D\text{-}N}^{water}$ (kcal/mol)[d]	15.58 ± 0.46	16.27 ± 1.78	6.88 ± 0.76	12.43 ± 0.42
$m_{D\text{-}N}^{kinetic}$[e]	2.99 ± 0.10	2.91 ± 0.63	2.52 ± 0.61	4.86 ± 0.44

[a]At 25 °C in 55 mM OM, 10 mM glycine (pH 10), and 2 mM EDTA. [b]Parameters refer to Scheme 1. D, I, and N are the denatured, intermediate, and native states, respectively; $K_I = [I]/[D]$, and k_f and k_u are refolding and unfolding rate constants, respectively. The values for K_I, k_f, and k_u are extrapolated to water using the corresponding m values that describe how the logarithms of these parameters vary with urea concentration. [c]Log $K_{D\text{-}N}^{water} = \log k_f^{water} + \log K_I^{water} - \log k_u^{water}$ (Scheme 1). [d]$\Delta G_{D\text{-}N}^{water} = -RT \ln(10) \times \log K_{D\text{-}N}^{water}$. [e]$m_{D\text{-}N}^{kinetic} = m_u - m_f - m_I$.

denaturation studies. In classical protein folding, this kinetic plot is consistent with Scheme 1:

$$D \underset{}{\overset{K_I}{\rightleftharpoons}} I \underset{k_u}{\overset{k_f}{\rightleftharpoons}} N \qquad \text{(Scheme 1)}$$

where I is an intermediate state that OmpA has to populate to fold to N, $K_I = [I]/[D]$, and k_f and k_u are refolding and unfolding rate constants, respectively.[27] The rollover is due to the accumulation of I at low denaturant concentrations. Note, however, that these kinetic data do not allow us to exclude an off-pathway scenario[28,29] in which the rollover derives from a species C from which OmpA has to unfold back to D to fold to N. On the basis of Scheme 1, we can derive the following equation to analyze our kinetic data:

$$\log k_{obs} = \log\left\{\left(10^{\log k_f + m_f[den]}\right)/\left[1 + 10^{-(\log K_I + m_I[den])}\right] + 10^{\log k_u + m_u[den]}\right\} \qquad (1)$$

where k_{obs} is the observed rate constant for folding or unfolding and the parameters m_f, m_I, and m_u describe how the microscopic parameters $\log k_f$, $\log K_I$, and $\log k_u$, respectively, depend linearly on urea concentration.[28,30] In Table 1, the values for K_I, k_f, and k_u are extrapolated to water using the corresponding m values. From these values, we may calculate a free energy of unfolding of 12.43 ± 0.42 kcal/mol, based on the relationships $\log K_{D\text{-}N}^{water} = \log k_f^{water} + \log K_I^{water} - \log k_u^{water}$ and $\Delta G_{D\text{-}N}^{water} = -RT \ln(10) \times \log K_{D\text{-}N}^{water}$. The term $m_u - m_I - m_f$ gives $m_{D\text{-}N}$, which describes the dependence of $\log K_{D\text{-}N}^{water}$ on GdmCl concentration. This value is 4.86 ± 0.44 M^{-1}, which is somewhat larger than the corresponding $m_{D\text{-}N}$ value from equilibrium studies (3.40 ± 0.53 and 3.73 ± 0.47 M^{-1}, respectively), but close within error.

The Folding−Unfolding Process of OmpA in Urea Is Multiphasic. We will now use these parameters to try to shed further light on the unfolding of OmpA in urea. Folding and unfolding of OmpA were followed over 0−3.5 and 5.5−8 M urea, respectively. Higher concentrations of urea were not accessible because of the dilution procedures involved in the refolding assay, while equilibrium processes were too slow between 3.5 and 5.5 M urea to be monitored reliably; at 3.5 and 5.5 M urea, the half-lives were around 30 h (comparable to values at the midpoint of unfolding in GdmCl). Data were fit to single-, double-, or triple-exponential decays (corresponding to fast, intermediate, and slow phases, respectively) as required. Examples of residuals from single, double, and triple fits are shown in Figure S2B of the Supporting Information. Triple exponentials were required only under conditions highly favorable to either the native (0−1.3 M urea) or denatured (6.5−8 M urea) state, while double exponentials sufficed in the region from 1.3−2 and 5.5−6.5 M urea and single exponentials between 2 and 3.5 M urea.

The results of our exponential fits are shown in Figure 3A−D where both rate constants and amplitudes are depicted. There are dramatic changes to both the rate constants (Figure 3A) and their associated amplitudes for refolding (Figure 3B) and unfolding (Figure 3C) throughout the process, but the total amplitudes of refolding and unfolding remain essentially constant throughout the measured concentration ranges. Thus, the whole population of OmpA changes from unfolded to folded (for folding experiments) and vice versa for unfolding experiments.

At low urea concentrations, refolding rates are characterized by three phases. The rate constant for the fast phase, which also makes the greatest contribution to the total amplitude throughout the whole refolding concentration range (Figure 3B), shows a curved decline with urea concentration, indicating a partially folded species as discussed for refolding in GdmCl. Neither the rate constants nor the amplitudes of the two slower phases change markedly with urea concentration, though there is a slight trend that the rate constant of the slowest phase actually increases with urea concentration (Figure 3A). For unfolding, the situation is much simpler. The rate constants of all three phases follow the same linear increase with urea concentration. There is, however, a distinct development in the associated amplitudes (Figure 3C). The amplitudes of both the intermediate and the slow phase decrease with an increasing urea concentration, the slow phase decreasing the most. In contrast, the amplitude of the fast phase increases linearly from 6.5 M urea onward.

Refolding of OmpA at low urea concentrations could be complicated by aggregation. SDS−PAGE is also able to detect oligomeric species of OmpA that tend to accumulate at surfactant concentrations close to the cmc.[31] However, our SDS−PAGE data do not indicate that such species occur during folding under these conditions, consistent with other reports that a low urea concentration maintains OmpA in a monomeric state.[32] Aggregation of protein would be expected to depend on protein concentration. We therefore refolded OmpA at five different concentrations between 0.2 and 2 μM in 0−2.5 M urea and 55 mM OM. We find that the total amplitude of the three refolding phases scales linearly with OmpA concentration

dx.doi.org/10.1021/bi300974y | Biochemistry 2012, 51, 8371−8383

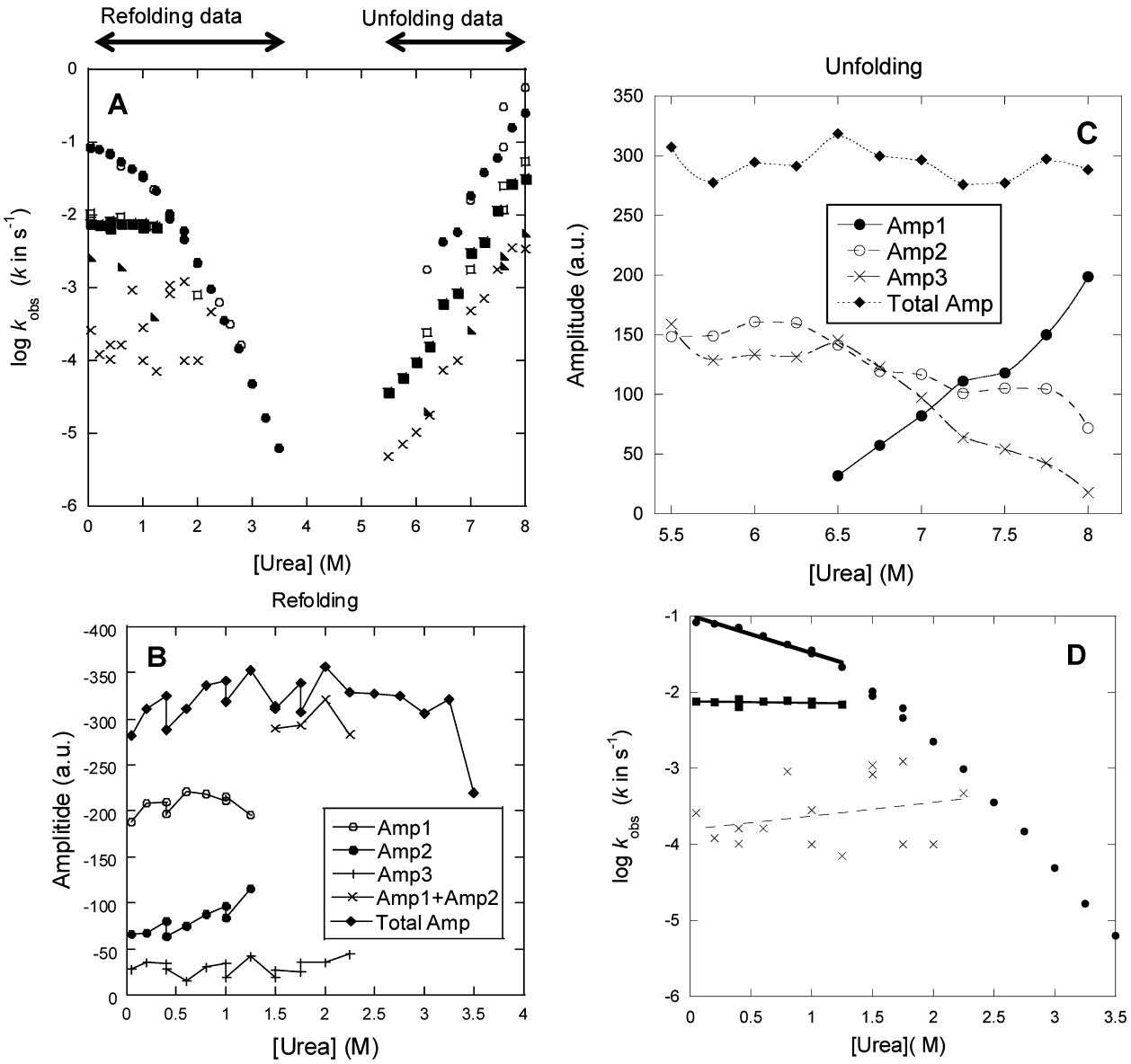

Figure 3. (A) Observed rate constants for folding and unfolding of FL-OmpA (filled symbols and ×) and TM-OmpA (empty symbols and triangles) in 55 mM OM vs urea concentration. For both constructs, up to three different relaxation phases are seen for both folding and unfolding. The associated amplitudes for FL-OmpA are shown for (B) refolding and (C) unfolding (note the symbols are not the same as in panel A; Amp1 corresponds to the fast phase, Amp2 to the middle phase, and Amp3 to the slow phase). For refolding, Amp1 and Amp2 can be distinguished only up to around 1.25 M urea, after which they merge. Errors were estimated to be 5%. The total amplitudes remain constant, but the different phases vary in intensity. (D) Close-up of the three different sets of refolding rate constants (for FL-OmpA only) from panel A, highlighting the different dependencies on urea concentration.

(Figure S3A,B of the Supporting Information). Moreover, the initial folding rates at different concentrations of OmpA are very similar (Figure S3C of the Supporting Information). These observations all indicate that aggregation is not a significant process during refolding in OM. The results also agree nicely with the observation by Moon and Fleming that surfactants may act as "holdases" to promote reversible refolding of outer membrane proteins and presumably avoid aggregation.[17]

Model for OmpA Refolding and Unfolding: A Single Intermediate. It is not easy to decide which of the three urea unfolding phases to adopt as the appropriate unfolding phase. In the interpretation provided in Discussion, we argue that the presence of several unfolding phases can be represented as parallel unfolding phases in which the native state is stripped of surfactant to different extents. In this model, the slowest phase represents unfolding from a ground state with the greatest amount of surfactant bound. Nevertheless, the amount of surfactant bound during refolding and unfolding will in any case differ, because there will be micelles during refolding but not during unfolding. Furthermore, use of the slow unfolding phase leads to a chevron plot with a minimum around 4.5 M urea (not shown), and this is considerably higher than the minimum of ~3.8 M urea predicted from the unfolding titration in Figure 1B. We also show below that for the "reduced" OmpA construct BBP, data fit much better to the fast unfolding phase than the slow unfolding phase. Finally, the use of the fast phase leads to data more consistent with GdmCl-derived data. Therefore, we classify the two slow refolding phases and two slow unfolding phases as parallel folding tracks and use the fast refolding and unfolding phases to represent the main pathway

dx.doi.org/10.1021/bi300974y | *Biochemistry* 2012, 51, 8371−8383

of folding and unfolding of OmpA in the presence of OM. As shown in Figure 4 and summarized in Table 1, the data fit very

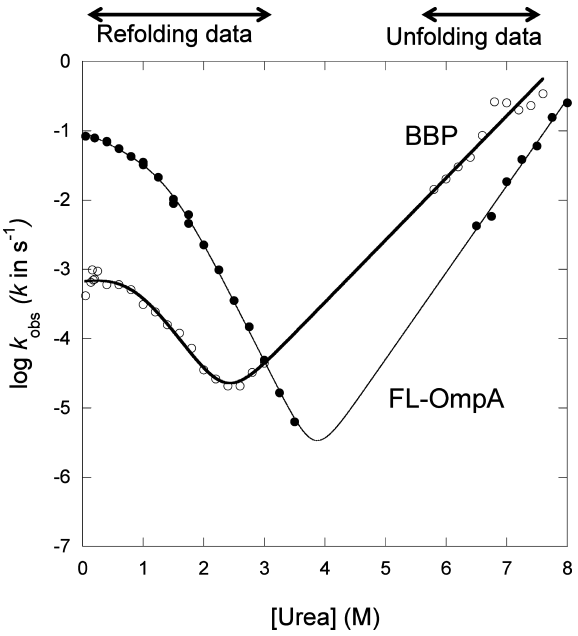

Figure 4. Rate constants assigned to the fast track of refolding and unfolding of FL-OmpA (●) and BBP (○) fit according to eq 1 derived from Scheme 1. The data are summarized in Table 1.

well to folding Scheme 1 and eq 1. Fitted values for FL-OmpA and TM-OmpA are identical within error. The minimum of the chevron plot, which also corresponds to the urea concentration where [N] = [U], is 3.8 ± 0.2 M, fully consistent with the pseudoequilibrium data in Figure 1B.

Comparison of kinetic data for Fl-OmpA folding in urea and GdmCl yields very similar refolding rates and the stability of the folding intermediate (Table 1), but unfolding rates are faster in GdmCl, extrapolating to a log value of −8.15 ± 0.12 (k in s^{-1}) in water, compared to −10.56 ± 0.31 for urea data. This leads to a slightly lower stability value for GdmCl compared to that for urea, despite the higher concentration of surfactant. Use of a stronger denaturant typically leads to higher extrapolated values of unfolding rates,[33−36] though the reasons for this are not clear.

Modulation of the OmpA Structure Can Strongly Destabilize It but Leads to Retention of the Overall Folding Pathway. In parallel with our studies with FL-OmpA, we also recorded the kinetics of refolding and unfolding of a transmembrane construct of OmpA (residues 1−176) at a limited number of urea concentrations. The purpose was to elucidate whether the C-terminal periplasmic domain (residues 177−325), which lacks Trp residues and therefore does not contribute to the folding signal, could influence folding kinetics in an indirect fashion. However, Figure 3A demonstrates complete overlay between data for OmpA and TM-OmpA (apart from a few of the rate constants for the slow refolding rate, which in any case are very scattered because of their small amplitude and low values). We conclude that our kinetic data truly record the behavior of the transmembrane barrel.

To elucidate the sensitivity of OmpA's parallel folding to changes in the sequence, we have compared the folding of FL-OmpA with that of the minimal transmembrane β-barrel platform (BBP). BBP is a derivative of OmpA from which the periplasmic domain has been removed and in which the four flexible surface-exposed extracellular loops of the TM domain of OmpA (containing 12, 11, 10, and 13 residues, respectively) are replaced with tight β-hairpin turns of one or two residues.[20] This does not prevent BBP from attaining the native state. Originally, BBP was successfully refolded from inclusion bodies in the presence of the surfactant phospholipid C_6PC at a surfactant concentration of ∼4 cmc.[20] The high (∼6 mg/mL) protein concentrations required for subsequent NMR studies required a multistep refolding approach to avoid misfolding and aggregation. We refold BBP at a final protein concentration of ∼16 μg/mL by simple dilution from 8 M urea into OM. Folding could be monitored by SDS−PAGE (Figure 5A), and superimposable titration curves could be attained in the folding and unfolding direction, with a midpoint of unfolding of ∼2.5 M urea (Figure 5B). Refolding was, however, not 100% complete. Even after incubation for several days, ∼20% of the protein remained in the unfolded state, suggesting that a significant proportion was trapped in a nonfoldable conformation (Figure 5A). Nevertheless, it was possible to exploit Trp fluorescence to follow BBP's rate of folding, which occurred orders of magnitude slower than for OmpA and TM-OmpA (Figure 5C). Refolding data were best fit to two-exponential decays, in which the amplitude of the slower phase declined and disappeared above 1 M urea (Figure 6A,B). A third slow phase could not be ruled out but was difficult to detect because of the extreme slowness of the reaction. Unfolding data could like those of OmpA be fit to three-exponential decays, where the fastest phase increased in amplitude with urea at the expense of the other two phases, and the slowest phase disappeared above 6.5 M urea (Figure 6A,B). The fast refolding rate constant showed the same rollover as for OmpA, while all three unfolding rate constants showed linear dependencies on urea concentration (Figure 6C).

The relative unfolding amplitudes could also be fit to Scheme 1 and eq 1 for shifts in the ground state populations, though the associated K_{ij} and m_{ij} values are significantly different from those of FL-OmpA (see the legend of Figure 6B and compare with Figure S4 of the Supporting Information). According to our model in Scheme 1, the removal of the extracellular loops has changed the binding of the surfactant molecules sufficiently to shift the relative stabilities of the ground state populations to a significant extent. (Note that this is just a model and that other factors may also be at play; there is no doubt that a dramatic shortening of the extracellular loops will affect loop entropy and thus affect overall kinetic and thermodynamic stability, but for the sake of simplicity, we focus on our simple scheme. The exact basis for the change in stability is not central to this report.) Using the same procedure that was used for OmpA, rate constants for the fast refolding and unfolding phase fit nicely to Scheme 1 with a minimum of ∼2.5 M urea (Figure 4), consistent with equilibrium denaturation data (Figure 5B). Use of the slower rate constants yielded poor fits and severely underestimated the m_u values. This vindicates the use of the fast refolding and unfolding rate constants for the analysis of OmpA folding.

However, BBP was destabilized at all levels compared to OmpA, leading to the lower stability of the intermediate, slower refolding from I to N, and faster unfolding of N. All in all, this accounted for a decrease in stability of almost 10 kcal/mol (Table 1). Thus, shortening of the extracellular loops severely reduces the stability of the protein but does not change the

dx.doi.org/10.1021/bi300974y | Biochemistry 2012, 51, 8371−8383

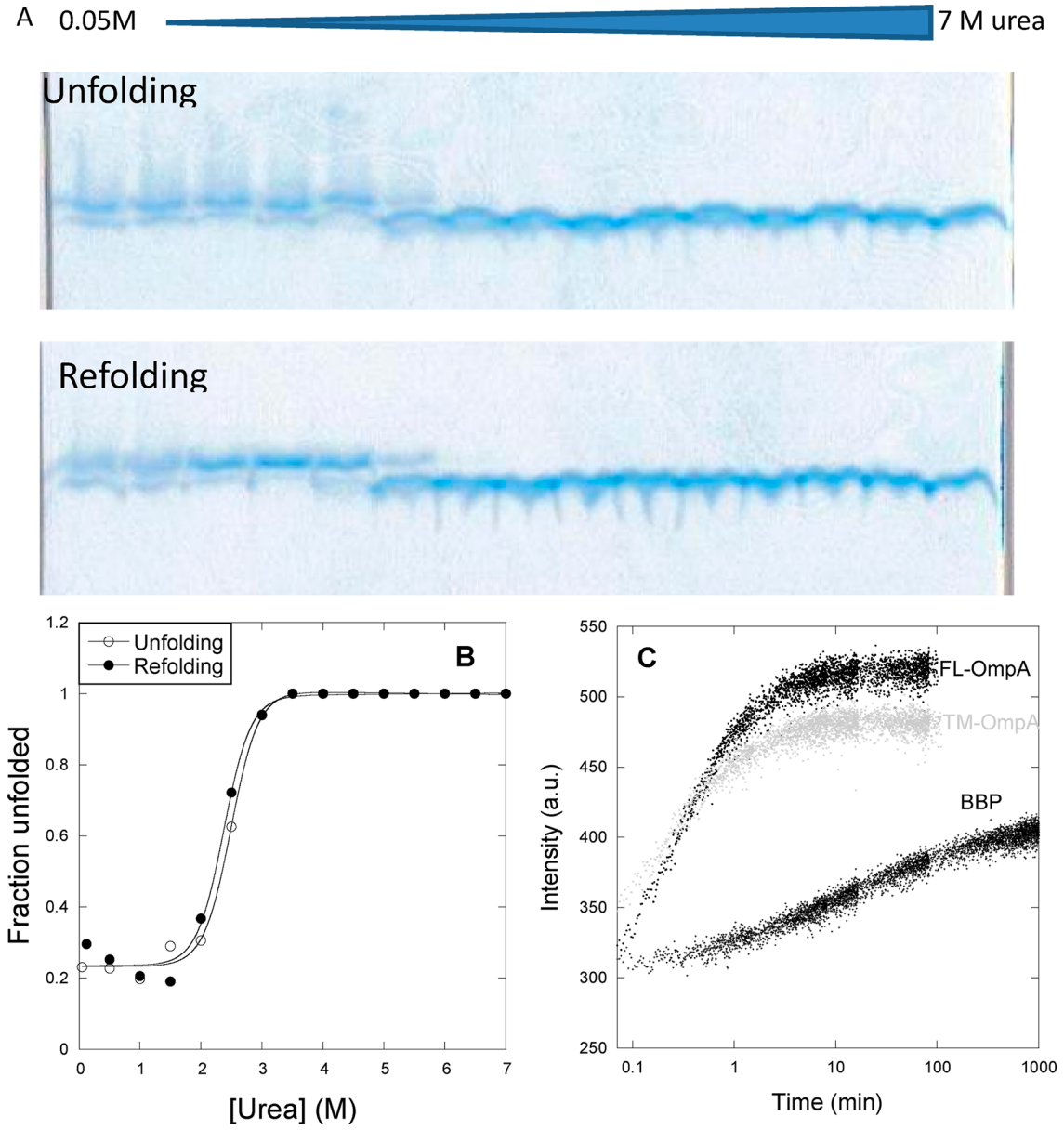

Figure 5. Folding of BBP compared to that of OmpA. (A) SDS−PAGE analysis of the refolding of BBP from 7 M urea and unfolding from 0.05 to 7 M urea after equilibration for 9 days. (B) Quantification of band intensities from panel A. Note that a significant fraction of BBP remains unfolded even at low urea concentrations. (C) Time profile for refolding of FL-OmpA, TM-OmpA, and BBP at 0.05 M urea. The apparent lag for BBP is an artifact of the logarithmic time axis.

overall folding scheme of OmpA. Note that the sum of the m_f, m_I, and m_u values for BBP is within error identical to that of FL-OmpA and TM-OmpA. The increased level of compaction of BBP through the removal of the extracellular loops clearly does not increase the m value. This presumably reflects the dynamic and flexible nature of the extracellular loops, which are essentially just as exposed in N as in D, so this removal does not alter the level of burial associated with folding.

DISCUSSION

Detection of Folding Intermediates. We have established that OmpA can refold and unfold reversibly at micellar concentrations of octyl maltoside in GdmCl and that the data are consistent with a single folding intermediate. The intermediate invoked in our model forms within the dead time of the mixing [and is not detected by stopped-flow kinetics (data not shown)] but forms only transiently. Detection of intermediates in the folding of OMPs is not an easy task, because SDS−PAGE usually does not provide information about stable intermediates. An exception was found for OmpA when it was folded in di-$C_{18:1}$PC vesicles. A band was observed within the first 30 min of the folding reaction migrating between the native and denatured band.[37] The band, however, accumulated only at 30 °C, not at higher (40 °C) or lower (20 °C) temperatures. Such an intermediate has not been detected with other vesicles with different lipid compositions or with surfactant micelles. Three intermediates have been identified in a more indirect fashion with time-resolved distance determinations by tryptophan fluorescence quenching (TDFQ).[9] This technique uses brominated lipids to quench tryptophan fluorescence as the protein penetrates and folds into the lipid bilayer. In di-$C_{18:1}$PC vesicles, three membrane-bound

dx.doi.org/10.1021/bi300974y | *Biochemistry* 2012, 51, 8371−8383

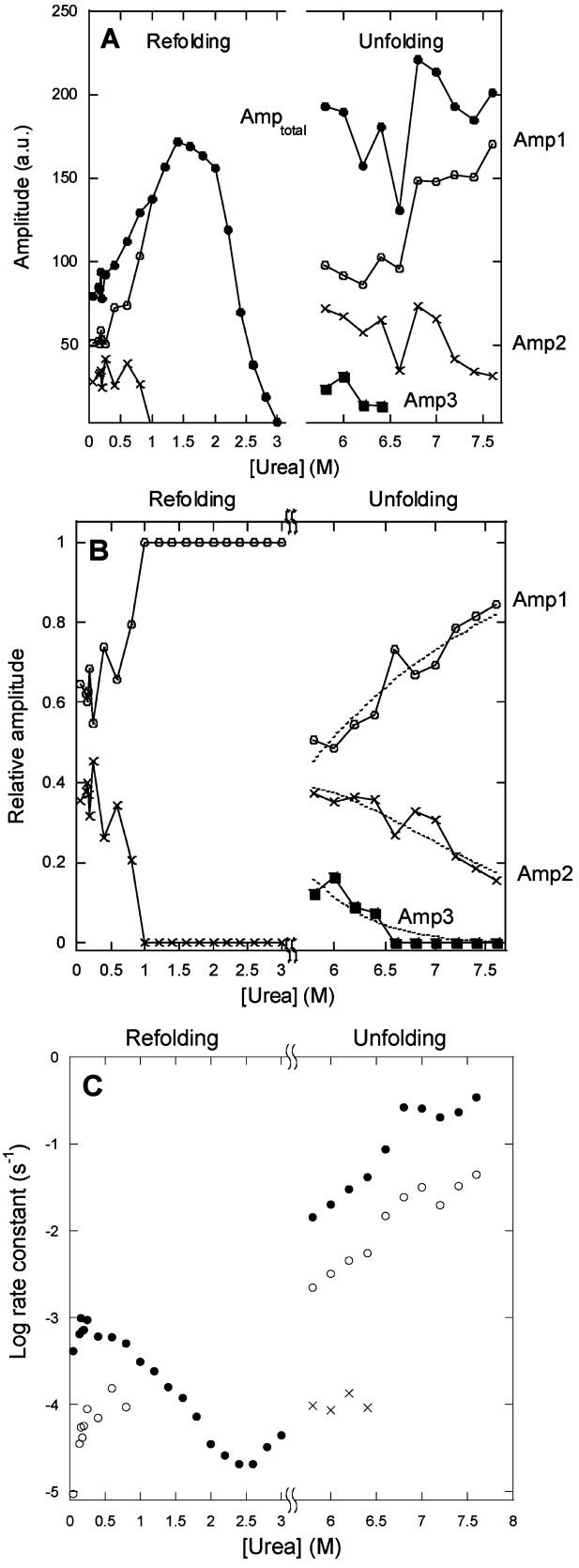

Figure 6. (A) Absolute and (B) relative amplitudes of refolding and unfolding of BBP. In panel B, relative amplitudes are analyzed as in Figure S5 of the Supporting Information. Best fits (stippled lines) are as follows: log K_{12}^{water} = 1.86, log K_{23}^{water} = 3.51, m_{12} = −0.33 M^{-1}, and m_{23} = −0.67 M^{-1}. (C) Rate constants for refolding and unfolding of BBP. See Figure 4 for a fit to Scheme 1.

intermediates were identified at different distances (14−16, 10−11, and 0−5 Å) from the center of the bilayer. Detection of the intermediates was temperature-dependent, so that the first intermediate was isolated at 2 °C, the second between 7 and 20 °C, and the third between 26 and 28 °C. The first intermediate was found to have disordered Trp residues, indicating that this intermediate had been adsorbed to the surface without a high degree of structure. The following intermediates develop more and more β-structure as the protein penetrates deeper into the bilayer. On the basis of the temperature dependence, the intermediate observed by SDS−PAGE (studied at 25 °C) may be similar to the third intermediate identified by TDFQ.[38] However, this suggestion can be verified in practice only by protein engineering, which probes the effects of different mutations on the folding behavior and energies of the different folding states.[39] Unfolding and refolding in GdmCl and OM provide a suitable framework for analyzing this process in detail. Such an approach will allow us to build up a detailed picture of the structure of folding intermediates and transition states at the level of individual side chains. Recent protein engineering studies of the folding of the α-helical proteins bacteriorhodopsin[40] and DsbB[41] and the β-barrel protein PagP[18] have shown this to be feasible for membrane proteins.

Multiphasic Folding Kinetics in Urea Suggest Parallel Pathways. Unfolding and refolding in urea are considerably more complex and slow than in GdmCl. Three relaxation phases are seen when OmpA unfolding in urea is monitored over time. The question of whether the three different folding phases in urea all relate to the same folding process now arises. That is, do they represent consecutive steps in one single pathway leading to the formation of N rather than parallel formation of N in three distinct pathways? We favor the parallel pathway scheme for two reasons.

First, all three refolding phases represent formation of monomeric N, as monitored by SDS−PAGE. This is the single most powerful indication that N is formed in several steps. In a single pathway, the native state would form in one phase, dictated only by the population of, and conversion from, the last intermediate preceding the native state. The interconversion of states preceding N will not be monitored by SDS−PAGE as only the native state is sufficiently stable to resist unfolding in SDS.

Second, the slopes of the refolding and unfolding limbs (m values) provide useful information about the change in compaction associated with a given folding step. For example, in a simple two-state folding scheme (D ↔ N) where no intermediates accumulate during folding, the m_f value describes the increase in the level of compaction from the ground state (D) to the transition state of folding (TS) while the m_u value describes the increase in the level of compaction from TS to N. Inspection of OmpA's kinetic m values shows that the overall change in compaction between the denatured and native states is not compatible with a consecutive folding scheme involving all three phases.[12,30] In the two-state folding scheme (D ↔ N), m_f and m_u must sum to the m value obtained from equilibrium unfolding experiments.[42] For more complicated schemes, the unfolding and refolding m values for different steps within a consecutive scheme must also sum to the equilibrium m value. In contrast, no such restrictions are required for parallel schemes.

We can estimate whether the m values are consistent with sequential or parallel folding as follows. While the data in Figure 1 do not represent a strict equilibrium, the apparent m

dx.doi.org/10.1021/bi300974y | Biochemistry 2012, 51, 8371−8383

values from the refolding data are around 2.4−2.9 M^{-1} over the 8 days we measure, providing a rough estimate of the expected *m* value. $m_{D\text{-}N}$ values in urea are typically only 50−75% of the corresponding values in GdmCl because of the latter's greater potency; this puts an upper limit of ∼1.9−2.7 M^{-1} on OmpA's $m_{D\text{-}N}$ value in urea. For the refolding rate constants, the *m* value associated with the linear stretch (1.5−3.5 M urea), which has a value of approximately −1.7 M^{-1}, reflects the change in compaction as we go from D to the main transition state, TS. The two slower refolding phases have *m* values close to zero. Conversely, the slopes of the three unfolding limbs represent changes in compaction on going from a ground state (e.g., N) to the TS. All three unfolding limbs have a slope of ∼1.3 M^{-1}. A consecutive folding scheme would require that the sum of all the *m* values (here around 5.6 M^{-1}) is equal to the sum of the equilibrium value, which is clearly not the case. By contrast, these *m* values are easily compatible with a parallel unfolding scheme in which a fast unfolding phase competes with two slower phases.

Parallel Folding Pathways May Reflect Early-Stage Surfactant Stripping. What is the origin of these parallel pathways? There are at least two possible explanations for parallel folding pathways, namely, peptidyl−prolyl isomerization and different levels of surfactant removal.

For *cis*−*trans* peptidyl−prolyl isomerization in the denatured state, only the fraction of the denatured state population with the peptidyl−prolyl bonds in the same *trans* conformation as the native state can fold directly to the native state.[43] For denatured protein molecules with peptidyl−prolyl bonds in the wrong (*cis*) conformation, the rate-limiting step in folding becomes the slow reconfiguration of the denatured state around the peptidyl−prolyl bond to a species with the same *trans* conformation as the native state.[43,44] The N-terminal domain of OmpA has six Pro residues, one in each of the four periplasmic loops, one exposed in a β-strand at the top of the barrel, and one in the C-terminus of the domain. The existence of *cis*−*trans* isomerization is often demonstrated by double-jump experiments in which N first unfolds and is then allowed to equilibrate for different lengths of time before refolding. The *cis*−*trans* states equilibrate relatively slowly, so there will be an only gradual increase in the amplitude of the slower phases.[45] We cannot exclude entirely the possibility that this isomerization plays a role in the formation of several refolding phases, as our N−D−N double jump experiments to investigate this did not yield clear data (data not shown). However, OmpA's slow refolding phases disappear at higher urea concentrations and show much lower m_f values than the fast phase. This is not easily reconciled with *cis*−*trans* isomerization that for other proteins persists alongside the main refolding reaction and with much the same *m* values, though they are shifted to considerably lower rate constant values.[44]

An alternative, though somewhat speculative, scenario is surfactant stripping. The slopes of the three folding limbs differ substantially. That of the fast phase is slightly negative; that of the intermediate phase is essentially zero, and that of the slow phase is slightly positive (Figure 3D). We would expect a negative slope from a folding process that leads to an increased level of compaction, because denaturants favor the less compact states[46] and therefore slow processes that lead to increased levels of compaction. In contrast, a horizontal line implies no change in compaction and a positive slope implies a decrease in the level of compaction. A simple reading of the changes in slope among the three phases is as follows. The fast phase represents a folding process accompanied by an increased level of compaction from the ground state to the TS; in the intermediate phase, the ground state and TS are equally compact, and in the slow phase, the TS is actually less compact than the ground state (cf. the impact of collapsed states on the refolding of globular proteins[29]). The folding process is initiated by the transfer of D into conditions favoring folding (low denaturant and high surfactant concentrations). In this transfer, D is generally thought to collapse to a more compact state because the folding conditions represent a poor solvent for the hydrophobic moieties of D.[47] We propose that D partitions into different states that are collapsed to different extents. The more collapsed states may represent folding detours or misfolded species that have to expand by unfolding again before folding can proceed. The extent of expansion will depend on the degree of misfolded collapse. Thus, in the fast phase, the ground state is not as highly collapsed as in the intermediate phase, which in turn is less collapsed than the slow phase. Further support for this suggestion comes from the observation that the amplitude of the fast phase declines in favor of the slow phase as we increase the temperature from 25 to 55 °C (Figure S5 of the Supporting Information). Higher temperatures favor collapse by promoting the hydrophobic effect. The slow phase is absent in GdmCl refolding, and the intermediate phase disappears at low concentrations (Figure 2); this is also consistent with a suppression of collapsed states because of a higher surfactant concentration in GdmCl (250 mM OM in GdmCl vs 55 mM OM in urea).

All three unfolding phases show a similar slope of ∼1.3 M^{-1}, indicating that they all involve the same change in compaction. However, the fast phase rises to prominence at higher urea concentrations where the amplitude of the slow phase gradually disappears while the intermediate phase declines to a smaller extent (Figure 3C). Thus, increasing urea concentrations clearly favor the fast phase. There are no OM micelles present in solution under unfolding conditions. This does not mean that OmpA is unable to bind OM at >3.2 M urea. Membrane proteins generally have a very high affinity for surfactants, exceeding that of surfactants for each other; otherwise, the proteins would not be able to attract surfactant molecules. Nevertheless, protein−surfactant interactions will weaken progressively with an increasing urea concentration, and at concentrations around 6−8 M urea, there will likely be very few protein−surfactant contacts. We interpret the change in the dominance of the different unfolding phases to mean that the fast phase represents an unfolding step in which the protein is stripped to its greatest extent of surfactant molecules in the initial stage of unfolding, so that unfolding proceeds from a "surfactant-deprived" but natively folded protein. More surfactant molecules will remain bound to OmpA in the intermediate phase, and even more in the slow phase. However, because the protein remains in N in the ground species for all three unfolding phases, the change in compaction between the ground state and the transition state is the same and hence the unfolding *m* value does not change.

This scenario is supported by an analysis of the relative values of the unfolding amplitudes that is consistent with a simple urea-driven partitioning between different ground states (see the Supporting Information and Figure S4). This model provides a straightforward equilibrium-based framework for the presence of several unfolded populations with differences in stability determined by urea (in combination with octyl maltoside). Furthermore, the partitioning of N into different

states with different levels of surfactant stripping is an instantaneous event that occurs as soon as the protein is folded (Figure S6 of the Supporting Information). The stabilizing role of OM against unfolding of OmpA in urea is documented by thermal scans (Figure S7 of the Supporting Information).

Additional support for the role of the surfactant in our stripping model is the fact that unfolding of OmpA in urea using 55 mM longer chain alkyl maltosides (decyl maltoside and dodecyl maltoside) is extremely slow even at the highest accessible urea concentration (9 M) (Figure S8 of the Supporting Information). Clearly, the longer the alkyl chain, the greater the affinity of the surfactant. Nevertheless, we emphasize that the model remains speculative and is supported only by circumstantial evidence.

Parallel Folding Pathways Are Also Seen in Other OMPs. Studying the folding mechanism of outer membrane proteins in membrane mimicking systems has primarily been performed using lipid vesicles produced by ultrasonication or by the use of extrusion through filters. Some of the proteins that have been most thoroughly studied are OmpA, FomA, and more recently PagP. Both OmpA and PagP have transmembrane β-barrel domains consisting of eight strands, while FomA is predicted to be a 14-strand β-barrel. The folding kinetics have been characterized for all three proteins in lipid vesicles, but their behaviors clearly differ. In lipid vesicles composed of short lipids (C_{10}–C_{12} alkyl chains), OmpA folding follows a single-step second-order rate law, involving binding of OmpA to lipid molecules that must be coupled to folding,[48] while folding in vesicles of longer lipids required two first-order (i.e., not directly lipid-binding) phases.[49] The folding of FomA is slower compard to that of OmpA, and folding occurs in at least two phases, irrespective of the lipid length.[38,49] Three phases are observed when folding PagP into lipid vesicles (di-C_{12}PC). A burst phase followed by two exponential phases was observed under conditions favoring the native state. Close to the transition point where N and D are equally stable, refolding kinetics were, however, satisfactorily described by a single phase, just as is seen for many globular proteins that accumulate intermediates only at low denaturant concentrations.[27,50] For OmpA and FomA, the fast phase (studied at only a single very low urea concentration) has been ascribed to a direct-track folding through rapid vesicle binding, while the slow phase has been attributed to a detour through hydrophobic collapse in an aqueous environment, which subsequently has to rearrange on the vesicle surface to fold.[38] This scenario corresponds to parallel rather than sequential folding events, and these conclusions are strongly substantiated by our own observations over a broad urea concentration range.

These parallel pathways probably stem from the specific properties of the denatured state of a membrane protein in the absence of a good solvent such as urea, given that such a state is highly prone to aggregation and will presumably therefore have a strong tendency to collapse in competition with binding to surfactant micelles. However, in the absence of such "distractions", folding of OmpA actually appears to be remarkably simple and involves only a single intermediate. Similarly, the existence of parallel unfolding pathways is also likely to reflect a peculiarity of the native state of the membrane protein, where surfactant stripping is required prior to unfolding. PagP is reported to unfold only in a single relaxation phase;[18] however, this occurs from a native state embedded in phospholipid vesicles, and it may behave differently if unfolded in the presence of surfactants instead. We speculate that PagP is so completely embedded in the phospholipid vesicle that unfolding requires very extensive dissolution of the vesicles from around the protein or another kind of dissociation of PagP from its membrane-inserted state, explaining the need for very high urea concentrations to effect unfolding. This would lead to only one ground state population (the essentially "naked" N state) prior to unfolding and only one relaxation phase.

Higher Stability of OMPs in Surfactants Than in Lipids. Our kinetic parameters from GdmCl- and urea-derived denaturation show that OmpA is highly stable in OM, as the native state is stabilized by 12–15 kcal/mol relative to the denatured state. This is considerably larger than the values of 3–7 kcal/mol observed by Hong and Tamm, by whom the thermodynamic stability of OmpA was assessed in lipid vesicles of different compositions. Obviously, neither surfactant micelles nor lipid vesicles are exact mimics of the actual environment of the outer membrane that has an asymmetric bilayer. While both phospholipid vesicles and surfactant micelles have macromolecular structures that can facilitate folding of outer membrane proteins, this study clearly demonstrates that different thermodynamic parameters can be obtained by the use of different model systems. In general, we must expect different levels of stability in vesicles[23] and surfactants[51] of different chain lengths and compositions. At the other extreme, Ohnishi and Kameyama used linear extrapolation methods from high temperatures and low SDS mole fractions in mixed SDS/octyl glucoside micelles[24] to show that OmpA unfolded ~1000 times faster in pure SDS micelles than it refolded, indicating that in SDS micelles the denatured state was ~4.4 kcal/mol more stable than the native state. Nevertheless, the unfolding half-life was ~4 years in SDS at 25 °C, in good agreement with the high activation barriers for unfolding that we and others have observed.

It is important to note that the remarkably high thermodynamic stability of OmpA calculated from the kinetic data reflects a very stable native state whose low energy consequently leads to a high barrier to unfolding. We are at present unable to explain the large difference between stabilities derived from data in a surfactant (this study) and vesicles.[23] Intuitively, one might expect lipids to stabilize OmpA to a greater extent in view of their close packing in the lipid bilayer and the good hydrophobic matching between lipid and protein, although it might also be argued that surfactants in view of their greater flexibility can pack better against OmpA. This might be particularly important in the loop region that appears to stabilize the protein strongly against unfolding. In vivo, the lipopolysaccharide molecules present in the outer leaflet may allow closer interactions and thus stabilize OmpA. However, a trivial possibility for the lipid–surfactant discrepancy is a methodological one, namely that equilibrium denaturation and SDS–PAGE analysis systematically underestimate the stability of OMPs. Kinetic rate constants and their dependence on denaturant concentration are determined with little error, allowing extrapolation over large concentration ranges provided the linear correlation is good. The overlap between re- and unfolding rate constants in GdmCl and their reasonable agreement with urea unfolding data further strengthen the use of this approach. In contrast, small changes in the degree of unfolding in the transition region (because of imperfect equilibration) can alter m values significantly and thus the stability. In view of the large challenges involved in obtaining

dx.doi.org/10.1021/bi300974y | Biochemistry 2012, 51, 8371–8383

reproducible equilibrium denaturation of outer membrane proteins in vesicles,[52,53] the possibility that hysteresis confounds the extraction of reliable parameters for denaturation of OmpA in vesicles cannot be excluded.[23]

■ ASSOCIATED CONTENT

Supporting Information

Information about the effect of urea on OM cmc values, the close correspondence between SDS−PAGE and Trp fluorescence for kinetic measurements and the goodness of different types of exponential fits, the independence of folding kinetics of OmpA concentration, a microscopic model of different ground states of unfolding, double-jump experiments showing instantaneous partitioning into different ground states, stabilization of OmpA by different concentrations of OM, and the slow unfolding of OmpA in alkyl maltosides with chains longer than those of OM. This material is available free of charge via the Internet at http://pubs.acs.org.

■ AUTHOR INFORMATION

Corresponding Author

*Telephone: +45 87 15 54 41. Fax: +45 86 12 31 78. E-mail: dao@inano.au.dk.

Author Contributions

K.K.A. and H.W. contributed equally to this work.

Funding

K.K.A. and D.E.O. were supported by a grant from the Danish Ministry of Science, Technology and Innovation to the innovation consortium BIOPRO. H.W. is supported by a predoctoral grant from Aarhus University, the Danish Research Training Council, Novozymes A/S, and Abbott Ltd. D.E.O. is supported by the Danish Research Foundation (inSPIN).

Notes

The authors declare no competing financial interest.

■ ACKNOWLEDGMENTS

We are very grateful to Dr. Konstantin Pervushin for generously donating the BBP expression plasmid.

■ ABBREVIATIONS

cmc, critical micelle concentration; D, denatured state; FL-OmpA, full-length OmpA (residues 46−370); I, intermediate state; LUV, large unilamellar vesicle; LPS, lipopolysaccharide; N, native state; OM, octyl maltoside; OmpA, outer membrane protein A from *E. coli*; SUV, small unilamellar vesicle; TM-OmpA, transmembrane domain of OmpA (residues 46−221).

■ REFERENCES

(1) Mogensen, J. E., and Otzen, D. E. (2005) Interactions between periplasmic chaperones and bacterial outer membrane proteins. *Mol. Microbiol. 57*, 326−346.

(2) Stanley, A. M., and Fleming, K. G. (2008) The process of folding proteins into membranes: Challenges and progress. *Arch. Biochem. Biophys. 469*, 46−66.

(3) Gu, J., Ji, X., Qi, J., Ma, Y., Mao, X., and Zou, Q. (2010) Crystallization and preliminary crystallographic studies of the C-terminal domain of outer membrane protein A from enterohaemorrhagic *Escherichia coli*. *Acta Crystallogr. 66*, 929−931.

(4) Grizot, S., and Buchanan, S. K. (2004) Structure of the OmpA-like domain of RmpM from *Neisseria meningitidis*. *Mol. Microbiol. 51*, 1027−1037.

(5) Surrey, T., and Jähnig, F. (1992) Refolding and oriented insertion of a membrane protein into a lipid bilayer. *Proc. Natl. Acad. Sci. U.S.A. 89*, 7457−7461.

(6) Surrey, T., and Jähnig, F. (1995) Kinetics of folding and membrane insertion of a β-barrel membrane protein. *J. Biol. Chem. 270*, 28199−28203.

(7) Kleinschmidt, J. H., and Tamm, L. K. (1996) Folding intermediates of a β-barrel membrane protein. Kinetic evidence for a multi-step membrane insertion mechanism. *Biochemistry 35*, 12993−13000.

(8) Kleinschmidt, J. H., den Blaauwen, T., Driessen, A. J. M., and Tamm, L. K. (1999) Outer membrane protein A of *Escherichia coli* inserts and folds into lipid bilayers by a concerted mechanism. *Biochemistry 38*, 5006−5016.

(9) Kleinschmidt, J. H., and Tamm, L. K. (1999) Time-resolved distance determination by tryptophan fluorescence quenching: Probing intermediates in membrane protein folding. *Biochemistry 38*, 4996−5005.

(10) Kleinschmidt, J. H., Wiener, M. C., and Tamm, L. K. (1999) Outer membrane protein A of *E. coli* folds into detergent micelles, but not in the presence of monomeric detergent. *Protein Sci. 8*, 2065−2071.

(11) Kleinschmidt, J. H., and Tamm, L. K. (2002) Secondary and tertiary structure formation of the β-barrel membrane protein OmpA is synchronized and depends on membrane thickness. *J. Mol. Biol. 324*, 319−330.

(12) Fersht, A. R. (1999) *Structure and mechanism in protein science. A guide to enzyme catalysis and protein folding*, Freeman & Co., New York.

(13) Lau, F. W., and Bowie, J. U. (1997) A method for assessing the stability of a membrane protein. *Biochemistry 36*, 5884−5892.

(14) Otzen, D. E. (2011) Protein-surfactant interactions: A tale of many states. *Biochim. Biophys. Acta 1814*, 562−591.

(15) Kleinschmidt, J. H., Wiener, M. C., and Tamm, L. K. (1999) Outer membrane protein A of *E. coli* folds into detergent micelles, but not in the presence of monomeric detergent. *Protein Sci. 8*, 2065−2071.

(16) Burgess, N. K., Dao, T. P., Stanley, A. M., and Fleming, K. G. (2008) β-Barrel proteins that reside in the *E. coli* outer membrane *in vivo* demonstrate varied folding behaviour *in vitro*. *J. Biol. Chem. 283*, 26748−26758.

(17) Moon, C. P., Kwon, S., and Fleming, K. G. (2011) Overcoming hysteresis to attain reversible equilibrium folding for outer membrane phospholipase A in phospholipid bilayers. *J. Mol. Biol. 413*, 484−494.

(18) Huysmans, G. H., Baldwin, S. A., Brockwell, D. J., and Radford, S. E. (2010) The transition state for folding of an outer membrane protein. *Proc. Natl. Acad. Sci. U.S.A. 107*, 4099−4104.

(19) Debnath, D., Nielsen, K. L., and Otzen, D. E. (2010) In vitro association of fragments of a β-sheet membrane protein. *Biophys. Chem. 148*, 112−120.

(20) Johansson, M. U., Alioth, S., Hu, K.-H., Walser, R., Koebnik, R., and Pervushin, K. V. (2007) A minimal transmembrane β-barrel platform protein studied by NMR. *Biochemistry 46*, 1128−1140.

(21) Surrey, T., and Jahnig, F. (1992) Refolding and oriented insertion of a membrane protein into a lipid bilayer. *Proc. Natl. Acad. Sci. U.S.A. 89*, 7457−7461.

(22) Abramoff, M. D., Magelhaes, P. J., and Ram, S. J. (2004) Image Processing with ImageJ. *Biophotonics International 11*, 36−42.

(23) Hong, H., and Tamm, L. K. (2004) Elastic coupling of integral membrane protein stability to lipid bilayer forces. *Proc. Natl. Acad. Sci. U.S.A. 101*, 4065−4070.

(24) Ohnishi, S., and Kameyama, K. (2001) *Escherichia coli* OmpA retains a folded structure in the presence of sodium dodecyl sulfate due to a high kinetic barrier to unfolding. *Biochim. Biophys. Acta 1515*, 159−166.

(25) Nozaki, Y., and Tanford, C. (1970) The solubility of amino acids, diglycine, and triglycine in aqueous guanidine hydrochloride solutions. *J. Biol. Chem. 245*, 1648−1652.

(26) Parker, M. J., Spencer, J., and Clarke, A. R. (1995) An integrated kinetic analysis of intermediates and transition states in protein folding reactions. *J. Mol. Biol. 253*, 771−786.
(27) Baldwin, R. (1996) On-pathway versus off-pathway folding intermediates. *Folding Des. 1*, R1−R8.
(28) Baldwin, R. L. (1997) Competing unfolding pathways. *Nat. Struct. Biol. 4*, 965−966.
(29) Otzen, D. E., and Oliveberg, M. (1999) Salt-induced detour through compact regions of the protein folding landscape. *Proc. Natl. Acad. Sci. U.S.A. 96*, 11746−11751.
(30) Mogensen, J. E., Ibsen, H., Lund, J., and Otzen, D. E. (2004) Elimination of an off-pathway folding intermediate by a single point mutation. *Biochemistry 43*, 3357−3367.
(31) Wang, H., Andersen, K., Vad, B. S., and Otzen, D. E. (2012) OmpA can form folded and unfolded oligomers. *Biochim. Biophys. Acta*, DOI: 10.1016/j.bbapap.2012.09.002.
(32) Ebie Tan, A., Burgess, N. K., DeAndrade, D. S., Marold, J. D., and Fleming, K. G. (2010) Self-association of unfolded outer membrane proteins. *Macromol. Biosci. 10*, 763−767.
(33) Otzen, D. E., and Fersht, A. R. (1998) Folding of circular and permuted chymotrypsin inhibitor 2: Retention of the folding nucleus. *Biochemistry 37*, 8139−8146.
(34) Mishra, R., Olofsson, L., Karlsson, M., Carlsson, U., Nicholls, I. A., and Hammarstrom, P. (2008) A conformationally isoformic thermophilic protein with high kinetic unfolding barriers. *Cell. Mol. Life Sci. 65*, 827−839.
(35) Huang, Q., and Quinones, E. (2008) Assessment of the stability and unfolding pathways of azurin from *Pseudomonas aeruginosa* through the combination of denaturating osmolytes. *Arch. Biochem. Biophys. 477*, 175−182.
(36) Sridevi, K., and Udgaonkar, J. B. (2002) Unfolding rates of barstar determined in native and low denaturant conditions indicate the presence of intermediates. *Biochemistry 41*, 1568−1578.
(37) Kleinschmidt, J. H., and Tamm, L. K. (1996) Folding intermediates of a β-barrel membrane protein. Kinetic evidence for a multi-step membrane insertion mechanism. *Biochemistry 35*, 12993−13000.
(38) Kleinschmidt, J. H. (2006) Folding kinetics of the outer membrane proteins OmpA and FomA into phospholipid bilayers. *Chem. Phys. Lipids 141*, 30−47.
(39) Fersht, A. R., Matouschek, A., and Serrano, L. (1992) The Folding of an Enzyme I: Theory of Protein Engineering Analysis of Stability and Pathway of Protein Folding. *J. Mol. Biol. 224*, 771−782.
(40) Curnow, P., and Booth, P. J. (2009) The transition state for integral membrane protein folding. *Proc. Natl. Acad. Sci. U.S.A. 106*, 773−778.
(41) Otzen, D. E. (2011) Mapping the folding pathway of the transmembrane protein DsbB by protein engineering. *Protein Eng., Des. Sel. 24*, 139−149.
(42) Jackson, S. E., and Fersht, A. R. (1991) Folding of chymotrypsin inhibitor 2. 1: Evidence for a two-state transition. *Biochemistry 30*, 10428−10435.
(43) Brandts, J. F., Halvorson, H. R., and Brennan, M. (1975) Consideration of the possibility that the slow step in protein denaturation reactions is due to cis-trans isomerism of proline residues. *Biochemistry 14*, 4953−4963.
(44) Jackson, S. E., and Fersht, A. R. (1991) Folding of chymotrypsin inhibitor 2. 2: Influence of proline isomerization on the folding kinetics and thermodynamic characterization of the transition state of folding. *Biochemistry 30*, 10436−10443.
(45) Otzen, D. E., and Oliveberg, M. (2001) A simple way to measure protein refolding rates in water. *J. Mol. Biol. 313*, 479−483.
(46) Timasheff, S. (2002) Protein hydration, thermodynamic binding, and preferential hydration. *Biochemistry 41*, 13473−13482.
(47) Dill, K. A., and Shortle, D. (1991) Denatured states of proteins. *Annu. Rev. Biochem. 60*, 795−825.
(48) Kleinschmidt, J. H., and Tamm, L. K. (2002) Secondary and tertiary structure formation of the β-barrel membrane protein OmpA is synchronized and depends on membrane thickness. *J. Mol. Biol. 324*, 319−330.
(49) Pocanschi, C. L., Apell, H. J., Puntervoll, P., Hogh, B., Jensen, H. B., Welte, W., and Kleinschmidt, J. H. (2006) The major outer membrane protein of *Fusobacterium nucleatum* (FomA) folds and inserts into lipid bilayers via parallel folding pathways. *J. Mol. Biol. 355*, 548−561.
(50) Matouschek, A., Kellis, J. T., Serrano, L., Bycroft, M., and Fersht, A. R. (1990) Transient folding intermediates characterized by protein engineering. *Nature 346*, 440−445.
(51) Andersen, K. K., and Otzen, D. E. (2009) How chain length and charge affect surfactant denaturation of ACB. *J. Phys. Chem. B 113*, 13942−13952.
(52) Moon, C. P., and Fleming, K. G. (2011) Side-chain hydrophobicity scale derived from transmembrane protein folding into lipid bilayers. *Proc. Natl. Acad. Sci. U.S.A. 108*, 10174−10177.
(53) Moon, C. P., and Fleming, K. G. (2011) Using tryptophan fluorescence to measure the stability of membrane proteins folded in liposomes. *Methods Enzymol. 492*, 189−211.